Nonlinear Dyn (2018) 94:977–989
https://doi.org/10.1007/s11071-018-4404-x

ORIGINAL PAPER

Dynamics of superregular breathers in the quintic nonlinear Schrödinger equation

Lei Wang · Chong Liu · Xuan Wu · Xin Wang · Wen-Rong Sun

Received: 13 January 2018 / Accepted: 1 June 2018 / Published online: 12 June 2018

Abstract In this paper, we consider an extended nonlinear Schrödinger equation that includes fifth-order dispersion with matching higher-order nonlinear terms. Via the modified Darboux transformation and Joukowsky transform, we present the superregular breather (SRB), multipeak soliton and hybrid solutions. The latter two modes appear as a result of the higher-order effects and are converted from a SRB one, which cannot exist for the standard NLS equation. These solutions reduce to a small localized perturbation of the background at time zero, which is different from the previous analytical solutions. The corresponding state transition conditions are given analytically. The relationship between modulation instability and state transition is unveiled. Our results will enrich the dynamics of nonlinear waves in a higher-order wave system.

Keywords The quintic nonlinear Schrödinger equation · Superregular breathers · Multipeak solitons · Hybrid solutions · State transition · Modulation instability

Lei Wang and Chong Liu are co-first authors.

L. Wang (✉) · X. Wu
Department of Mathematics and Physics, North China Electric Power University, Beijing 102206, People's Republic of China
e-mail: wanglei2239@126.com

C. Liu (✉)
School of Physics, Northwest University, Xi'an 710069, People's Republic of China
e-mail: nwudavid@163.com

C. Liu
Shaanxi Key Laboratory for Theoretical Physics Frontiers, Xi'an 710069, People's Republic of China

X. Wang
College of Science, Zhongyuan University of Technology, Zhengzhou 450007, People's Republic of China

W.-R. Sun
School of Mathematics and Physics, and Beijing Key Laboratory for Magneto-Photoelectrical, Composite and Interface Science, University of Science and Technology Beijing, Beijing 100083, People's Republic of China

1 Introduction

Wave evolution in different physical fields is governed by the nonlinear partial differential equations [1–14]. Though the nonlinear Schrödinger (NLS) equation contains only the lowest-order dispersion and lowest-order nonlinearity, it can well describe the propagation and dynamics of nonlinear pulses in diverse physics, including water waves [15], nonlinear optics [16], plasma [17], Bose–Einstein condensates [18,19] and several other cases. The integrability of this equation [20] enables us to get such analytical solutions as solitons, breathers [21] and rogue waves [22–31], which have been observed in numerous experiments in these areas [32–37]. In many cases, the dynamics of a system influenced by modulation instability (MI) is also described by the NLS equation. In particular, there are some special interests on the nonlinear evolution stage and long-time dynamics, which are beyond the linear stability analysis. Zhakarov and Gelash [38,39] proposed a kind of breather solution of the NLS equation, namely the superregular breather (SRB) solution. They further claimed that the SRB solution starts with infinitesimally small localized perturbation and could be used to describe the nonlinear stage of MI [38–40]. The SRBs are unique nonlinear wave structures on a plane-wave background formed by a nonlinear superposition of pairs of quasi-Akhmediev breathers [38–40]. This unique feature has been observed in both optics and hydrodynamics, based on exact superregular breather solution of the standard NLS equation [40]. However, in order to claim that one has characterized the nonlinear stage of MI, one must study solutions generated by generic initial conditions [41,42]. Biondini and Mantzavinos [41,42] have studied the nonlinear stage of the MI by characterizing the initial value problem for the focusing NLS equation with nonzero boundary conditions at infinity. As shown in [41], for generic perturbations of the background, the signature of MI lies precisely in the portion of the continuous spectrum which is the nonlinearization of the unstable Fourier modes. In fact, it was also shown in [41] that there are classes of initial conditions that are modulational unstable but that do not generate any discrete spectrum. These classes include small localized perturbations of the background. Since these perturbations generate no discrete spectrum, they do not produce SRBs. Moreover, as shown in [42], small localized perturbations of the background lead to a universal wedge-shaped structure. Asymptotically in time, the spatial domain divides into three regions: a far left and a far right field, in which the solution is approximately equal to its initial value, and a central region in which the solution has oscillatory behavior described by slow modulations of the periodic traveling wave solutions [42].

The above studies show that the NLS equation is a good candidate describing various physical mechanisms in different contexts. Nevertheless, to increase the wave amplitude, we have to consider the higher-order effects which do not exist in the simplest NLS equation [43]. In studies of pulse propagation in optical fibers, for transmitting the ultrashort pulses whose durations are shorter than 100 fs, the higher-order effects such as the third-order dispersion, self-steepening and delayed nonlinear response have to be taken into account. Thus, it is necessary to study the other integrable models of the whole hierarchy except for the NLS equation. Two extensions of the hierarchy to third- and fourth-order terms are known as the Hirota equation [44] and Lakshmanan–Porsezian–Daniel (LPD) equation [45–48]. More recently, the quintic equation of the hierarchy has been studied by Hoseini and Marchant [49]. The quintic nonlinear Schrödinger (QNLS) equation reads as [50–53],

$$i\,q_t + S[q(x,t)] - i\,\varepsilon\,Q[q(x,t)] = 0, \tag{1.1}$$

where $S[q(x,t)]$ is the second-order NLS operator,

$$S[q(x,t)] = \tfrac{1}{2}q_{xx} + q|q|^2, \tag{1.2}$$

while $Q[q(x,t)]$ is the fifth-order quintic operator,

$$\begin{aligned} Q[q(x,t)] = {} & q_{xxxxx} + 10|q|^2 q_{xxx} + 10(q|q_x|^2)_x \\ & + 20q^* q_x q_{xx} + 30|q|^4 q_x. \end{aligned} \tag{1.3}$$

and ε is an arbitrary real parameter and can be varied and set close to an experimental value. This flexibility allows us to make reasonable adjustments for the actual physical phenomenon to be approximated in future experiments. Here x is the propagation variable, and t is the transverse variable (time in a moving frame). The function $|q(x,t)|$ is the envelope of the waves. A series of works on this equation have been done including the Darboux transformation [50], conservation laws [51], breather solutions [52], and breather-to-soliton conversions [53].

Well recent studies suggest that advanced improvement in NLS equation could lead to some qualitatively new characteristics for rogue waves and breathers [54,55]. Increasing the value of higher-order terms causes the observation of the compression effects of the breathers in the LPD equation [56]. These effects could make the rogue wave twisted in the Sasa–Satsuma equation [57–59]. The state transitions among breathers and other types of nonlinear waves such as the multipeak soliton, anti-dark soliton, periodic wave and W-shaped soliton can appear as a result of the existence of the higher-order effects [53,60–67]. And the rogue waves can be also converted into the W-shaped solitons [68,69]. In particular, the higher-order effects affect the MI, the growth rate of which shows a nonuniform distribution characteristic in the low perturbation frequency region and opens up a stability region as the background frequency changes [63–69].

In the present work, based on the QNLS equation, we mainly concentrate the dynamics of the SRB solutions and their state transition induced by the fifth-order effects. By means of the Darboux transformation, we first show that the SRB solutions still exist in the NLS equation in spite of the fifth-order dispersion with matching higher-order nonlinear terms. Further, we transform the SRBs into the multipeak solitons while keep the small localized perturbation unchanged. Such transition occurs under a special condition where the radial and angle satisfy a transition equation. The transformed solitons are expected to be observed in future optical experiments. We finally reveal the relationship between transformed soliton and linear MI.

2 The SRB solutions and state transitions

In this section, via the Darboux transformation and method in Refs. [38,39], we discuss the characteristics of the SRB solutions for the QNLS equation. Due to the fifth-order dispersion with matching higher-order nonlinear terms, we show that the SRB solutions can be transformed into other two types of ones, i.e., the multipeak soliton solution and hybrid solution.

2.1 The SRB solutions

Equation (1.1) is the compatibility condition for the following overdetermined linear system for a matrix function Ψ [50]

$$\begin{aligned}\Psi_x &= U\Psi = (\lambda U_0 + U_1)\Psi,\\ \Psi_t &= V\Psi = \begin{pmatrix} A & B \\ -B^* & -A \end{pmatrix}\Psi,\end{aligned} \tag{2.1}$$

with U and V being 2×2 matrices,

$$\begin{aligned}\Psi =&(\varphi,\psi)^{\mathrm{T}},\\ U_0 =&\begin{pmatrix} -i & 0 \\ 0 & i \end{pmatrix}, \qquad U_1 = \begin{pmatrix} 0 & q \\ -q^* & 0 \end{pmatrix},\\ A =& -16i\lambda^5\varepsilon + 8i\lambda^3\varepsilon|q|^2\\ &+4\lambda^2\varepsilon\left(qq_x^* - q_xq^*\right) - i\lambda^2\\ &-2i\lambda\varepsilon\left(qq_{xx}^* + q^*q_{xx} - |q_x|^2 + 3|q|^4\right)\\ &+\frac{1}{2}i|q|^2\\ &+\varepsilon\left(q^*q_{xxx} - qq_{xxx}^* + q_xq_{xx}^* - q_{xx}q_x^*\right.\\ &\left.+6|q|^2q^*q_x - 6|q|^2q_x^*q\right),\\ B =&16\lambda^4\varepsilon q + 8i\lambda^3\varepsilon q_x - 4\lambda^2\varepsilon\left(q_{xx} + 2|q|^2q\right)\\ &-2i\lambda\varepsilon\left(q_{xxx} + 6|q|^2q_x\right) + \lambda q\\ &+\varepsilon\left(q_{xxxx} + 8|q|^2q_{xx}\right.\\ &\left.+2q^2q_{xx}^* + 4|q_x|^2q + 6q_x^2q^* + 6|q|^4q\right)\\ &+\frac{1}{2}iq_x,\end{aligned}$$

where λ is an eigenvalue parameter and φ and ψ are two linear complex functions. Using the Darboux transformation, we can give the N-order solutions of Eq. (1.1)

$$q^{[n]} = q^{[0]} - 2i\frac{\Delta_1}{\Delta}, \tag{2.2}$$

with

$$\Delta_1 = \begin{vmatrix} \varphi_1 & \psi_1 & \cdots & \lambda_1^{n-2}\varphi_1 & \lambda_1^{n-2}\psi_1 & \lambda_1^{n-1}\varphi_1 & \lambda_1^{n}\varphi_1 \\ \varphi_2 & \psi_2 & \cdots & \lambda_2^{n-2}\varphi_2 & \lambda_2^{n-2}\psi_2 & \lambda_2^{n-1}\varphi_2 & -\lambda_2^{n}\varphi_2 \\ \vdots & \vdots & \vdots & \vdots & \vdots & \vdots & \vdots \\ \varphi_{2n} & \psi_{2n} & \cdots & \lambda_{2n}^{n-2}\varphi_{2n} & \lambda_{2n}^{n-2}\psi_{2n} & \lambda_{2n}^{n-1}\varphi_{2n} & -\lambda_{2n}^{n}\varphi_{2n} \end{vmatrix},$$

$$\Delta = \begin{vmatrix} \varphi_1 & \psi_1 & \cdots & \lambda_1^{n-2}\varphi_1 & \lambda_1^{n-2}\psi_1 & \lambda_1^{n-1}\varphi_1 & \lambda_1^{n-1}\psi_1 \\ \varphi_2 & \psi_2 & \cdots & \lambda_2^{n-2}\varphi_2 & \lambda_2^{n-2}\psi_2 & \lambda_2^{n-1}\varphi_2 & \lambda_2^{n-1}\psi_2 \\ \vdots & \vdots & \vdots & \vdots & \vdots & \vdots & \vdots \\ \varphi_{2n} & \psi_{2n} & \cdots & \lambda_{2n}^{n-2}\varphi_{2n} & \lambda_{2n}^{n-2}\psi_{2n} & \lambda_{2n}^{n-1}\varphi_{2n} & \lambda_{2n}^{n-1}\psi_{2n} \end{vmatrix}.$$

Hereby, $q^{[0]}$ is a certain particular solution of Eq. (1.1) and $\Psi_j = (\varphi_j, \psi_j)^{\mathrm{T}}$ are the fundamental matrix solutions of Lax Pair (2.1). Choosing N complex numbers λ_j corresponding to Ψ_j, we can obtain the new solution of Eq. (1.1) by Expression (2.2).

In order to obtain the breather solutions, we consider the plane-wave solution $q^{[0]} = c\,\mathrm{e}^{i\,(a\,x+b\,t)}$ as the initial one, where c, b and a represent the amplitude, wave number and frequency, respectively. Further, to facilitate the SRB solutions, we perform the Joukowsky transform to λ as follows

$$\lambda = -i\frac{c}{2}\left(\xi + \frac{1}{\xi}\right) - \frac{a}{2}, \qquad \xi = R\,\mathrm{e}^{i\,\alpha}, \tag{2.3}$$

which maps the plane of λ onto the outer part of the circle of unit radius. The parameters R (radius) and α (angle) are the polar coordinates of the point. Then, the first-order breather solution can be written in the following form ($n = 1$):

$$q_B^{[1]} = c\left(1 - 2\left(R + \frac{1}{R}\right)\cos\alpha\,\frac{\varphi_1\psi_1^*}{|\varphi_1|^2 + |\psi_1|^2}\right) q^{[0]}, \tag{2.4}$$

with

$$\varphi_1 = \frac{e^{A - i\alpha}}{R} + e^{-A}, \psi_1 = \frac{e^{-A - i\alpha}}{R} + e^{A},$$
$$A = hx + \omega t + \frac{1}{2}(\mu - i\theta),$$
$$h = h_R + i h_I = \frac{c}{2}\left(R - \frac{1}{R}\right)\cos\alpha + i\frac{c}{2}\left(R + \frac{1}{R}\right)\sin\alpha,$$
$$\omega = h(\omega_R + i\omega_I) = h\left[2a^4\varepsilon - 4a^3\lambda_1\varepsilon + 8a^2\varepsilon\left(\lambda_1^2 - 3c^2\right) + a\left(24c^2\lambda_1\varepsilon - 16\lambda_1^3\varepsilon - 1\right) + 2\left(6c^4\varepsilon - 8c^2\lambda_1^2\varepsilon + \lambda_1 + 16\lambda_1^4\varepsilon\right)\right],$$
$$\lambda_1 = -\frac{a}{2} + \frac{c}{2}\left(R - \frac{1}{R}\right)\sin\alpha - i\frac{c}{2}\left(R + \frac{1}{R}\right)\cos\alpha,$$
$$h_R = \frac{c}{2}\left(R - \frac{1}{R}\right)\cos\alpha, h_I = \frac{c}{2}\left(R + \frac{1}{R}\right)\sin\alpha,$$
$$\omega_R = 2(-a + 5a^4\varepsilon - 40a^2c^2\varepsilon + 16c^4\varepsilon) - c(R - R^{-1})(1 - 20a^3\varepsilon + 50ac^2\varepsilon)\sin\alpha + 4c^2(-5a^2 + 3c^2)(R^2 + R^{-2})\varepsilon\cos 2\alpha - 10ac^3(R^3 - R^{-3})\varepsilon\sin 3\alpha + 2c^4(R^4 + R^{-4})\varepsilon\cos 4\alpha,$$
$$\omega_I = -c(R + R^{-1})(1 - 20a^3\varepsilon + 50ac^2\varepsilon)\cos\alpha - 4c^2(-5a^2 + 3c^2)(R^2 - R^{-2})\varepsilon\sin 2\alpha - 10ac^3(R^3 + R^{-3})\varepsilon\cos 3\alpha - 2c^4(R^4 - R^{-4})\varepsilon\sin 4\alpha,$$

In Eq. (2.4), the parameters θ and μ, respectively, define the location and phase of the breather. The group velocity and phase velocity of the breather can be given by

$$V_{\text{ph}} = -\frac{h_R\,\omega_I}{h_I} - \omega_R, \quad V_{\text{gr}} = -\omega_R + \frac{h_I\,\omega_I}{h_R}. \tag{2.5}$$

Similarly, the second-order breather solution via Expression (2.2) can be given by ($n = 2$)

$$q_B^{[2]} = c\left(1 - i\left(R^2 - \frac{1}{R^2}\right)\sin 2\alpha\,\frac{N_R + iN_I}{\Delta}\right) e^{i\rho}, \tag{2.6}$$

with

$$N_R = \left(R + \frac{1}{R}\right)\cos\alpha\left[\left(|\psi_1|^2 - |\varphi_1|^2\right)\varphi_2\psi_2^* + \left(|\varphi_2|^2 - |\psi_2|^2\right)\varphi_1\psi_1^*\right],$$
$$N_I = -\left(R - \frac{1}{R}\right)\sin\alpha\left[\left(|\psi_1|^2 + |\varphi_1|^2\right)\varphi_2\psi_2^* + \left(|\varphi_2|^2 + |\psi_2|^2\right)\varphi_1\psi_1^*\right],$$
$$\Delta = \sin^2\alpha\left(R - \frac{1}{R}\right)^2(|\varphi_1|^2|\varphi_2|^2 + |\psi_1|^2|\psi_2|^2) + 4\cos^2\alpha(|\varphi_1|^2|\psi_2|^2 + |\psi_1|^2|\varphi_2|^2) - \cos^2\alpha\left(R + \frac{1}{R}\right)^2(\varphi_1\psi_2\psi_1^*\varphi_2^* + \psi_1\varphi_2\varphi_1^*\psi_2^*) + \left(R - \frac{1}{R}\right)^2(|\varphi_1|^2|\psi_2|^2 + |\psi_1|^2|\varphi_2|^2),$$
$$\varphi_1 = \frac{e^{A_1 - i\alpha}}{R} + e^{-A_1}, \psi_1 = \frac{e^{-A_1 - i\alpha}}{R} + e^{A_1},$$
$$A_1 = hx + \omega t + \frac{1}{2}(\mu_1 - i\theta_1),$$
$$\varphi_2 = \frac{e^{A_2 - i\alpha}}{R} + e^{-A_2}, \psi_2 = \frac{e^{-A_2 - i\alpha}}{R} + e^{A_2},$$
$$A_2 = h^* x + \omega^\star t + \frac{1}{2}(\mu_2 - i\theta_2),$$

$$\omega^\star = h^*(\omega_R^\star + i\omega_I^\star) = h^*\left[2a^4\varepsilon - 4a^3\lambda_2\varepsilon + 8a^2\varepsilon\left(\lambda_2^2 - 3c^2\right) + a\left(24c^2\lambda_2\varepsilon - 16\lambda_2^3\varepsilon - 1\right) + 2\left(6c^4\varepsilon - 8c^2\lambda_2^2\varepsilon + \lambda_2 + 16\lambda_2^4\varepsilon\right)\right].$$

In fact, solution (2.6) includes two sets of parameters R_j, α_j, θ_j and μ_j for $j = 1, 2$. Hereby, we only consider the case $R_1 = R_2 = R$ and $\alpha_1 = -\alpha_2 = \alpha$ for the SRBs in opposite directions. This is depicted in Fig. 1.

Solutions (2.4) and (2.6) describe different types of nonlinear waves depending on the values of the parameters R and α. The case $R > 1$ and $\alpha = 0$ is response for the Kuznetsov–Ma breather, while $R = 1$ and $\alpha \neq 0$ give rise to the Akhmediev breather. When $\alpha \to 0$, solution (2.4) describes the Peregrine rogue wave. In addition, we set $R = 1 + \sigma$ (σ is a small parameter), which could lead to the observation of quasi-annihilation at the moment of collision. Conversely, the case $R = 1$ will cause two Akhmediev breathers with opposite values of angular parameter completely annihilate each other. In order to illustrate the effect of

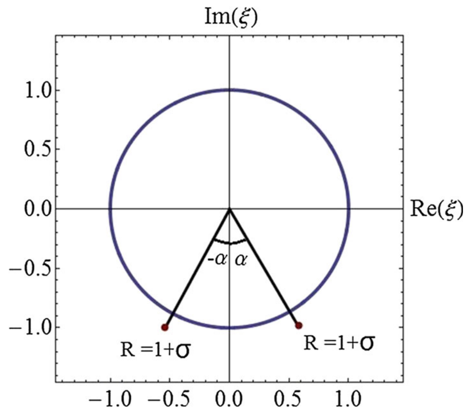

Fig. 1 (Color online) Uniformization of symmetrical eigenvalue parameters of second-order breather with the help of Joukowsky transform with the same small parameter σ and symmetrical angle α

R on the breather more clearly, Fig. 2 is plotted to show the conversion process from a Akhmediev breather ($R = 1$) to a quasi-Akhmediev breather ($R = 1.2$) to a general breather ($R = 1.5$) as the value of R grows. Two additional phase-shift parameters θ and μ affect the shape and amplitude of the perturbation. The degree of complexity of the wave profile at the area of collision depends on the difference between $\theta_1 + \theta_2$ and π. For example, the most effective annihilation appears when $\theta_1 + \theta_2$ approaches π. This will allow us to observe the SRBs. For the detailed discussion of the effects of parameters θ and μ, one can refer to Refs. [38,39].

In Fig. 3a, we display the first-order breather solution of the QNLS equation with $R = 1.13$, $\alpha = 0.6$, $\mu_{1,2} = 0$, $c = 1$, $a = 0.5$ and $\varepsilon = 0.1$. This type of solution is periodic in neither time nor space while it is periodic along the line connecting the peak maxima. Figure 3b describes the ghost interaction of breathers. The collision point is just another maximum of either breather solution. Each breather then appears seemingly without influence of the collision process. Figure 3c characterizes the synchronized collision between two SRBs from which we can observe a second-order rogue wave at the origin. Figure 3d is plotted for the quasi-annihilation of SRBs at the origin. Such phenomena correspond to the cases $\theta_{1,2} = 0$, $\theta_{1,2} = \frac{\pi}{2}$ and $\theta_{1,2} = \pi$, respectively. And $\mu_{1,2} = 0$, $R = 1.13$ and $\alpha = 0.6$ for all cases. Hereby, we are particularly focused on the last interaction since it has more physical and practical significance. It is well known that the Akhmediev breathers develop from periodic perturbations in Benjamin–Feir instability that require the whole infinite space [40]. While the two quasi-Akhmediev breathers reduce to a small localized perturbation (LP) of the background at time zero, which is shown in Fig. 4 clearly. Further, the perturbation $\delta q = 1-q^{[2]}$ on the continuous wave can be approximated by

$$\delta q = q_B^{[2]} - c\,e^{i\,\rho} \approx 4\,i\,c\,\sigma\,\frac{\cosh\,(i\,\alpha + 2\,V_G\,h_R t)\cos(2\,\sin\alpha\,x - \frac{\theta_1-\theta_2}{2})}{\cosh(2\,\sigma\,x\,\cos\alpha)}, \tag{2.7}$$

the temporal width of which increases with decreasing σ, whereas the amplitude decreases. This means that

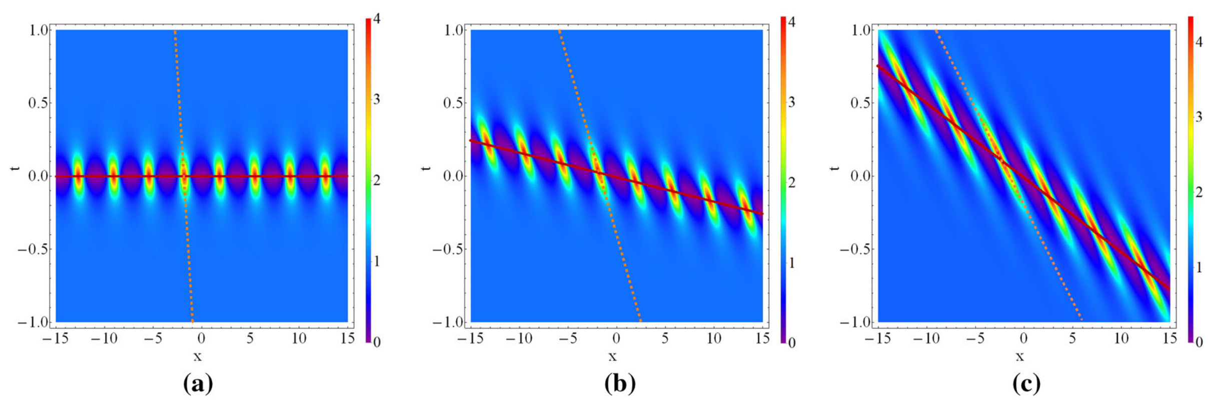

Fig. 2 (Color online) Intensity distribution of fundamental modes ($I = |q|^2$) with the same α ($=\pi/3$) as $R \to 1.5$. **a** Akhmediev breather ($R = 1$), **b** quasi-Akhmediev breather ($R = 1.2$), **c** general breather ($R = 1.5$). The solid lines represent the group velocity $V_{\rm gr}$, while the dashed lines describe the phase velocity $V_{\rm ph}$

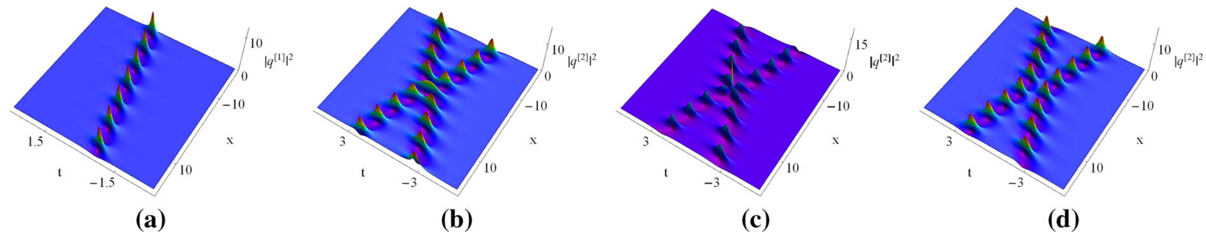

Fig. 3 (Color online) Intensity distribution ($I = |q|^2$) of a first-order quasi-AB and the three modes of second-order breather solution ($R = 1.13$, $\alpha = 0.6$, $\mu_{1,2} = 0$, $c = 1$, $a = 0.5$ and $\varepsilon = 0.1$) with the following phase shifts: **b** ghost case: $\theta_{1,2} = 0$, **c** amplification case: $\theta_{1,2} = \pi$, **d** superregular case: $\theta_{1,2} = \frac{\pi}{2}$. Notice that the amplitudes $|q^{[2]}(0,0)|^2$ are **b** 5.4104, **c** 18.7145, **d** 1.1636, respectively

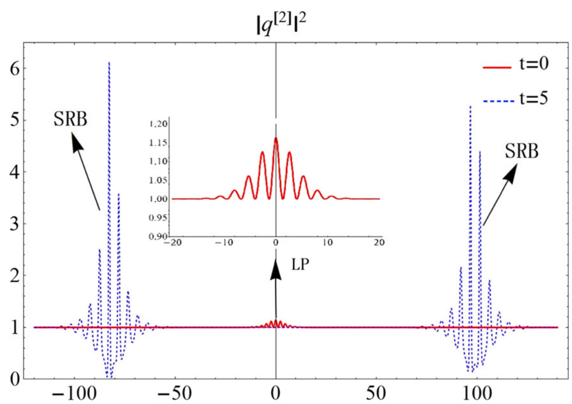

Fig. 4 (Color online) The development of the quasi-annihilation of breathers with the same parameters as in Fig. 3d. Red solid line is small perturbation at the moment $t = 0$. Blue dashed line is the breathers solution at the moment $t = 5$

the small parameter σ plays an important role in the LP. Note that δq possesses a perturbed frequency $2\sin\alpha$.

Despite the fifth-order dispersion and nonlinearity terms, the SRB solutions still exist in the QNLS equation. Additionally, these terms have no influence on the small LP, at first glance. However, as previous studies pointed out, the higher-order effects can lead to the state transition between breather and soliton [53,60,62–64]. Therefore, we will expect to observe some new phenomena in next part.

2.2 The multipeak soliton solution

As shown in Ref. [53], the breathers can be converted into solitons when the fifth-order dispersion parameter ε, real part λ_r, and imaginary part λ_i of the eigenvalue satisfy the following equation [53]

$$\begin{aligned} &2\,\varepsilon[a^3 - 4\,a^2\lambda_r - 2\,a(3\,c^2 - 6\,\lambda_r^2 + 2\,\lambda_i^2) \\ &\quad + 8\lambda_r(c^2 - 4\,\lambda_r^2 + 4\,\lambda_i^2)] = 1 \qquad i = 1, 2. \end{aligned} \tag{2.8}$$

Here, Eq. (2.8) is formulated in polar coordinate form to facilitate the transformation. To convert two quasi-Akhmediev breathers into solitons completely, we use two different sets of values of the radius and angle as follows

$$\begin{aligned} &R_1 = 1 + \sigma_1, \quad R_2 = 1 + \sigma_2, \\ &\sigma_1 \neq \sigma_2, \quad \alpha_1 \neq -\alpha_2. \end{aligned} \tag{2.9}$$

In this case, Eq. (2.8) can be expressed in forms of

$$\begin{aligned} \varepsilon = R_i^3 \Big/ \Big[&4\sin(\alpha_i)\left(2R_i^2\left(R_i^2 - 1\right)\left(5a^2 - c^2 - 2\right) - 1\right) \\ &+ 10aR_i\left(2R_i^2\left(a^2 - c^2 - 2\right) + R_i^4 + 1\right) \\ &- 4R_i\left(R_i^4 - R_i^2 + 1\right)\cos(2\alpha_i)(5a + 2R_i\sin(\alpha_i)) \\ &+ 4\sin(3\alpha_i)\Big], \quad i = 1, 2. \end{aligned} \tag{2.10}$$

Equation (2.10) is the state transition equation in polar coordinates. It includes four important parameters, namely the radius R, the angle α, the frequency a and the higher-order term ε. Thus, for the given ε and a, we can realize the state transition by the manipulation of the other two parameters R_i and α_i. On the other hand, one can easily check that Eq. (2.10) is equivalent to the condition

$$V_{\mathrm{gr},i} = V_{\mathrm{ph},i}, \qquad i = 1, 2. \tag{2.11}$$

Interestingly, Eq. (2.11) suggests that the transformed solitons appear as a result of the case where the group

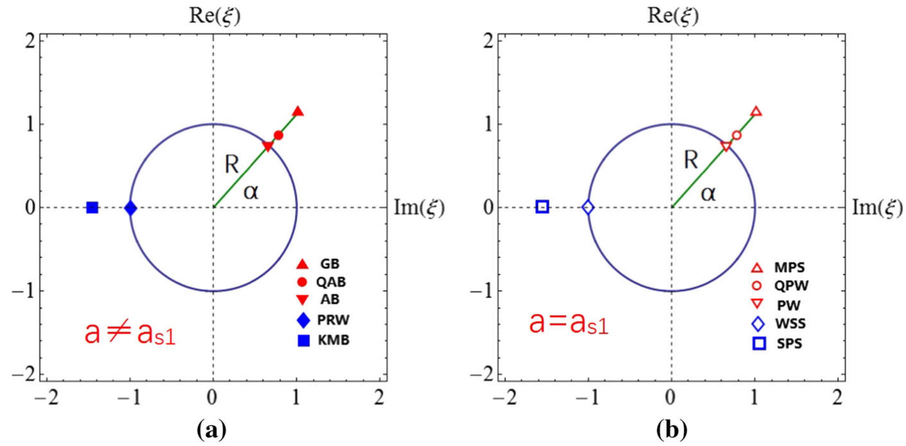

Fig. 5 (Color online) Phase diagrams of fundamental nonlinear modes in the Re(ξ)–Im(ξ) plane ($\xi = R\mathrm{e}^{i\alpha}$) with (**a**) $a \neq a_{s1}$ and (**b**) $a = a_{s1}$. **a** shows well-known breathing modes including "GB" (general breather), "QAB" (quasi-Akhmediev breather),"AB" (Akhmediev breather), "KMB" (Kuznetsov–Ma breather), and "PRW" (Peregrine rogue wave), while for the same pole (i.e., the same R, α), **b** displays non-breathing modes including "MPS" (multipeak soliton), "QPW" (quasiperiodic wave), "PW" (periodic wave), "SPS" (single-peak soliton), and "WSS" (W-shaped soliton)

velocity and phase velocity of the SRB solution have an equal value. Note that both $V_{\mathrm{gr},i}$ and $V_{\mathrm{ph},i}$ are related to the frequency a that can be flexibly adjusted. So we can satisfy condition (2.11) by controlling the value of a. Solving Eq. (2.11), we obtain the values of $a_i = a_{s,i}$ for $i = 1, 2$. For the fixed R_i, α_i and ε, using $a_i = a_{s,i}$ in Eq. (2.10) will lead to the conversion between the SRBs and solitons. Therefore, we have different routes to realize the state transition by the manipulation of the eigenvalue (R_i, α_i) or the frequency a. Similar to the case in Refs. [63,64], the solitons also have different types of nonlinear modes with the corresponding eigenvalues. Hereby, we demonstrate the phase diagrams of fundamental nonlinear modes in Fig. 5.

The independence of the two sets of eigenvalue parameters (R_i and α_i, $i = 1, 2$) allows us to conveniently control the two transformed solitons. But these two eigenvalue parameters should be associated with the same values of ε and a. Each set of R_i and α_i meeting Eq. (2.10) can turn a SRB into a multipeak soliton. However, we have to require the amplitude of the small LP almost unchanged after the conversion except for its shape. This means that not all values of R_i and α_i are suitable for transformations. Only the R_i and α_i whose values do not significantly increase the amplitude of the small LP can be considered. On the other hand, the two quasi-Akhmediev breathers are required to have different group velocity to prevent the overlap. In addition to R and α, one can find the group velocity is related to three other parameters, namely a, c and ε. The parameter c denotes the background amplitude and is generally taken as 1 while ε is a system parameter. Consequently, we mainly control the group velocity of the two SRBs by adjusting the value of the frequency a. The condition

$$V_{\mathrm{gr},i} = V_{\mathrm{gr},j}, \quad i \neq j. \tag{2.12}$$

will result in the overlap of two SRBs which have been studied in Ref. [60]. Solving Eq. (2.12) with respect to a, we have $a = a_f$. We omit this case since it does not involve LP. Instead, under the condition

$$V_{\mathrm{gr},i} \approx V_{\mathrm{gr},j}, \qquad i \neq j, \tag{2.13}$$

the group velocity of one of solitons is closed to that of another one. This could allow us to observe some novel nonlinear modes in the nonlinear stage of MI. Therefore, we consider the case $a \approx a_f$. It should be pointed out that we fail to obtain a_f analytically due to the computational complexity. However, we show how the parameter a affects the group velocity and phase velocity in Fig. 6. Conditions (2.11), (2.12) and (2.13), respectively, correspond to the cases $a = a_{s,i}$, $a = a_f$, and $a \approx a_f$. So in conclusion, we can choose the suitable value of the frequency a to manipulate the dynamics of the SRBs and solitons.

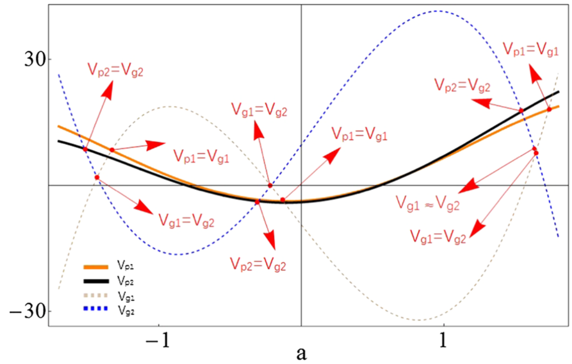

Fig. 6 (Color online) Evolution of $V_{\mathrm{gr},i}$ and $V_{\mathrm{ph},i}$ $(i = 1, 2)$ with a. The conditions $V_{\mathrm{gr},i} = V_{\mathrm{ph},i}$, $V_{\mathrm{gr},i} = V_{\mathrm{gr},j}$ and $V_{\mathrm{gr},i} \approx V_{\mathrm{gr},j}$, respectively, correspond to the cases $a = a_{s,i}$, $a = a_f$, and $a \approx a_f$

As mentioned, the solution of Eq. (2.10) is complicated and has to be found numerically. Solving Eq. (2.10) for a fixed values of ε and a (for example $\varepsilon = -0.049$ and $a = 0.5$) provides us with two solutions, i.e., $R_1 = 1.03$, $\alpha_1 = 0.6$ and $R_2 = 1.08$, $\alpha_2 = 0.715$. In this case, the two transformed solitons have the similar velocity but they do not overlap. The corresponding wave profile is shown in Fig. 7a from which we observe that two quasi-Akhmediev breathers are converted into the stable multipeak solitons in the same direction over a period of time. Fig. 7b depicts a global scene of collision between two multipeak solitons clearly. The fifth-order dispersion and nonlinear term inhibit the periodic oscillations of the SRBs during their propagations. We also note that these two solitons have the same propagation direction, which breaks the limit of definition of SRB in opposite directions in Refs. [38,39]. Unfortunately, we have not found the transformed solitons with different directions since this case will produce a larger LP. Such case is worth further study. Another interesting phenomenon is that a beating pattern appears before the formation of the multipeak solitons, which is depicted in Fig. 8a. The beating patterns are formed by the nonlinear superposition of two general breathers, as reported in Refs. [52,60]. This occurs when the directions of propagation of the two colliding breathers coincide. Nevertheless, the velocities of two waves in Fig. 7a are similar but not identical. Thus, the beating pattern is different from the previous ones and shows the feature of the short-lived life. As shown in Fig. 8b, at the branch point (BP), the beating structure is beginning to divide into two multipeak solitons. It is difficult to give the position of this point analytically. It may be associated with the separation distance between the two waves. Hereby, we define the position of the BP on which two main peaks of the solitons are formed and present its coordinate numerically ($t = 141.14$, $x = 213.47$).

2.3 The hybrid solution

In this part, we are concerned with another type of state transition that only involves one multipeak soliton. In this case, the eigenvalue parameters meet the following condition

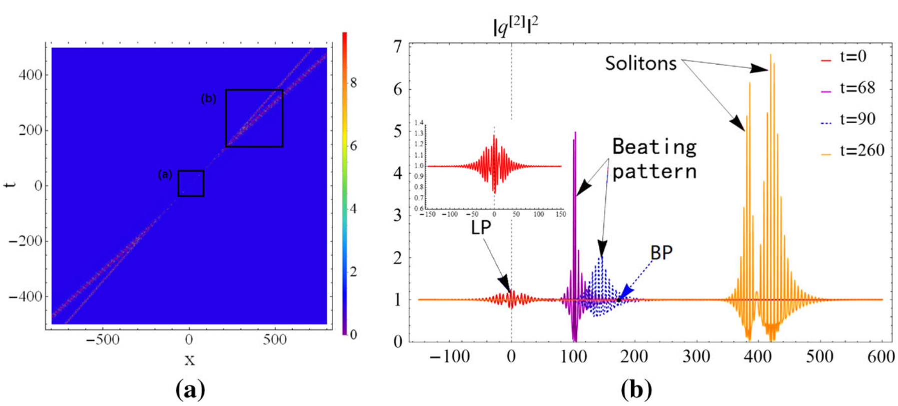

Fig. 7 (Color online) **a** The quasi-annihilation of two multipeak solitons (they have the similar velocities) propagating in same directions with $R_1 = 1.03$, $R_2 = 1.08$, $\alpha_1 = 0.6$, $\alpha_2 = 0.715$, $\mu_{1,2} = 0$, $\theta_{1,2} = \frac{\pi}{2}$, $c = 1$, $a = 0.5$ and $\varepsilon = -0.049$. **b** is the global scenario of development of a small localized perturbation. A small localized perturbation experiences two major phases of developments, i.e., the beating pattern and two multipeak soliton state

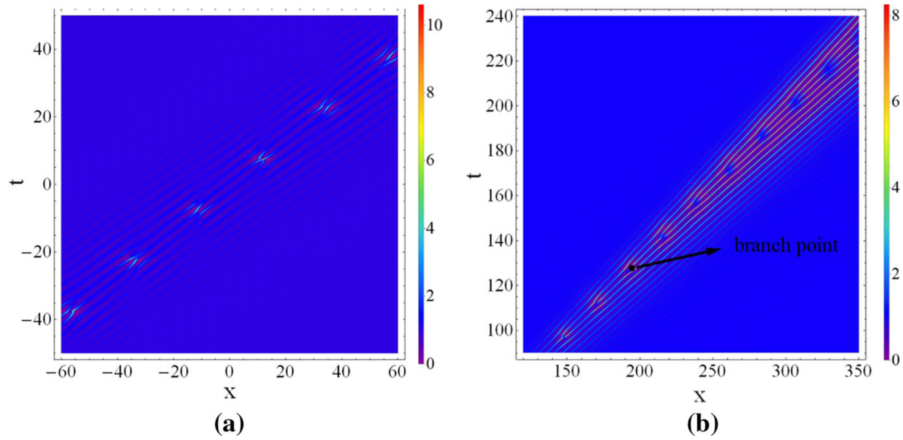

Fig. 8 (Color online) **a** The beating pattern [area A in enlarged Fig. 7a]. **b** The BP [area B in enlarged Fig. 7a]

$$R_1 = R_2 = R = 1 + \sigma, \qquad \alpha_1 = -\alpha_2 = \alpha. \tag{2.14}$$

The above relation indicates that the two sets of parameters (R_j, α_j) for $j = 1, 2$ relate to each other. The values of the radiuses are equal, while the angles are antisymmetric. Consequently, if one of quasi-Akhmediev breathers is converted into a soliton, then the other one cannot be transformed. The governing equation for such transition is given by

$$\begin{aligned}\varepsilon = R^3 \Big/ \Big[& 4\sin(\alpha)\left(2R^2\left(R^2-1\right)\left(5a^2-c^2-2\right)-1\right) \\ & + 10aR\left(2R^2\left(a^2-c^2-2\right)+R^4+1\right) \\ & - 4R\left(R^4-R^2+1\right)\cos(2\alpha)(5a+2R\sin(\alpha)) \\ & + 4\sin(3\alpha)\Big],\end{aligned} \tag{2.15}$$

which is equivalent to the following relation

$$V_{\mathrm{ph},1} = V_{\mathrm{gr},1}. \tag{2.16}$$

As depicted in Fig. 9, one can observe the collision between a stable multipeak soliton and a breather with fast group velocity in opposite directions. The two waves reduce to a small localized perturbation of the background at time zero as before. This again confirms the fact that the higher-order effects can lead to more nonlinear wave patterns. In addition, by selecting the suitable values of R_i and α_i for $i = 1, 2$, we could observe other types of nonlinear waves such as the antidark solitons, W-shaped solitons and M-shaped solitons in the nonlinear stage of MI.

3 The relation between state transition and linear MI

To reveal the relation between the state transition and linear MI, we perform the linear stability analysis of the background wave $q^{[0]}$ via adding small-amplitude perturbed Fourier modes p, i.e., $q_p = [c+p]\mathrm{e}^{i\rho}$, where $p = f_+\mathrm{e}^{i(\Lambda x - \Omega t)} + f_-^*\mathrm{e}^{-i(\Lambda x - \Omega^* t)}$ with small amplitudes f_+, f_-^*, perturbed frequency Λ, and wave number

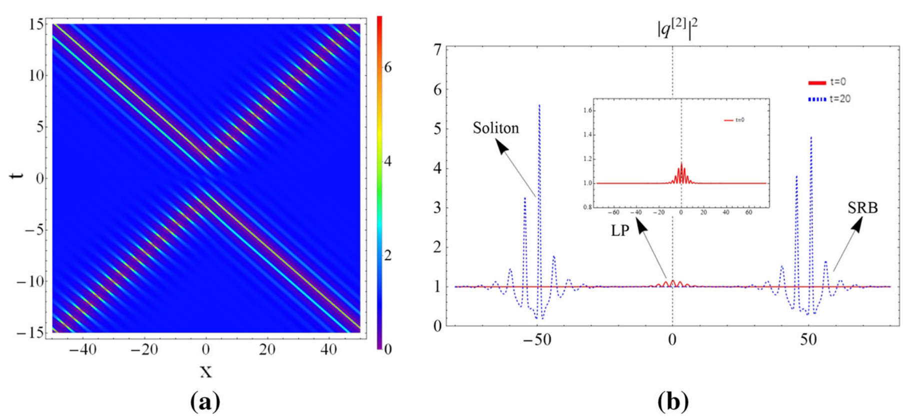

Fig. 9 Quasi-annihilation of a multipeak soliton and a superregular breather with $R_1 = R_2 = 1.13$, $\alpha_1 = -\alpha_2 = 0.6$, $\mu_{1,2} = 0$, $\theta_{1,2} = \frac{\pi}{2}$, $c = 1$, $a = -0.1271$ and $\varepsilon = 0.1$. **b** is the cross-sectional view of **a** at $t = 0$ and $t = 20$

Ω. Substituting the perturbed solution q_p into Eq. (1), followed by the linearization process in Refs. [68,69], leads to the following dispersion relation

$$\begin{aligned}\Omega =&\Lambda\,[a-5\,a^4\,\epsilon+10\,a^2\,\epsilon\,(6\,c^2-\Lambda^2)\\&-\epsilon\,(30\,c^4-10\,c^2\,\Lambda^2+\Lambda^4)]\\&\pm\frac{\sqrt{\Lambda^2-4\,c^2}}{2}\Big|\Lambda[1-10\,a\,\epsilon(2\,a^2-6\,c^2+\Lambda^2)]\Big|.\end{aligned} \tag{3.1}$$

MI exists when $\mathrm{Im}(\Omega) > 0$ (thus MI exists in the region $\Lambda < 2c$ with $\Lambda[1-10\,a\,\epsilon(2\,a^2-6\,c^2+\Lambda^2)] \neq 0$) and is described by the growth rate $G = k\,\mathrm{Im}(\Omega) > 0$, where $k > 0$ is a real number. Namely, a small-amplitude perturbations in this case suffer MI and grow exponentially like $\exp(G\,t)$ at the expense of pump waves.

As mentioned, δq possesses a perturbed frequency $\Lambda = 2\sin\alpha$ which belongs to the linear MI region $|\Lambda| < 2$. Conversely, the MI is absent and the small perturbation cannot be amplified. In addition, the transformed solitons generated from the SRB solutions have close relations with the linear MI in the presence of higher-order effects. Figure 10 shows the MI growth rate distribution with $\varepsilon \neq 0$. It is obviously found that the higher-order effects affect the distribution characteristic of MI growth rate in the subregion $-2 < \Lambda < 2$. There are three asymmetric modulation stability (MS) regions where the corresponding MI growth rate is equal to zero. Further, the MS regions can be given analytically by

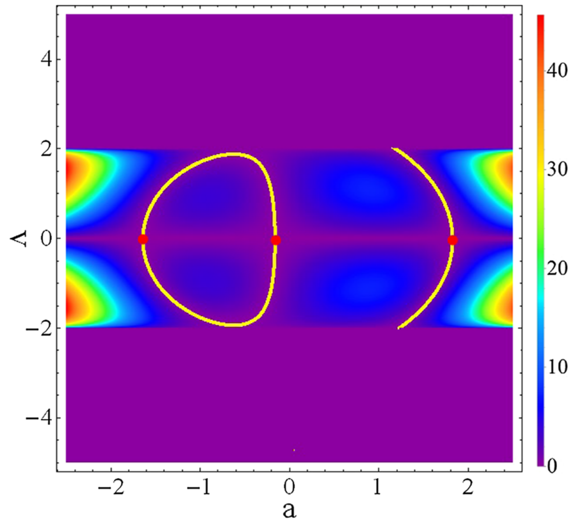

Fig. 10 (Color online) Distribution of linear MI growth rate $G = k\,\mathrm{Im}(\Omega) > 0$ on (Λ, a) plane with $c = 1$, $\epsilon = 0.1$, $k = 2$. The abscissa values of the red points in (10) correspond to three roots of Eq. (3.3), namely a_j for $j = 1, 2, 3$

$$\epsilon=\frac{1}{10\,a\left(2\,a^2-6\,c^2+\Lambda^2\right)}, \tag{3.2}$$

which is shown by the solid lines in Fig. 10. If the value of Λ in Eq. (3.2) is closed to zero, we have

$$\epsilon=\frac{1}{10\,a\left(2\,a^2-6\,c^2\right)}. \tag{3.3}$$

Solving Eq. (3.2) with respect to a, we have

$$a_1=-\frac{1}{2}\left(\frac{4\times 5^{\frac{1}{3}}\,c^2\epsilon}{M^{\frac{1}{3}}}+\frac{M^{\frac{1}{3}}}{5^{\frac{1}{3}}\,\epsilon}\right), \tag{3.4a}$$

$$a_2=\frac{5^{\frac{1}{3}}\,(1+i\,\sqrt{3})\,c^2\epsilon}{M^{\frac{1}{3}}}+\frac{(1-i\,\sqrt{3})\,M^{\frac{1}{3}}}{4\times 5^{\frac{1}{3}}\,\epsilon}, \tag{3.4b}$$

$$a_3=\frac{5^{\frac{1}{3}}\,(1-i\,\sqrt{3})\,c^2\epsilon}{M^{\frac{1}{3}}}+\frac{(1+i\,\sqrt{3})\,M^{\frac{1}{3}}}{4\times 5^{\frac{1}{3}}\,\epsilon}, \tag{3.4c}$$

with

$$M=-\epsilon^2+\sqrt{\epsilon^4-1600\,c^6\epsilon^6}.$$

Interestingly, state transition condition (2.8) can also be converted into Eq. (3.3) as we consider the rogue wave eigenvalue $\lambda = -\frac{a}{2} + c\,i$. In this case, the SRBs are transformed into the W-shaped solitons. This indicates that the W-shaped solitons appears in a MS region where the perturbation frequency satisfies $\Lambda = 0$ and the frequency of the background wave $a = a_j$ for $j = 1, 2, 3$ [also see the red points in Fig. 10].

4 Conclusions

To conclude, we have studied the dynamics of SRB solutions governed by the QNLS equation that includes the fifth-order dispersion with matching higher-order nonlinear terms. We have shown that the SRB solutions can also exist for the QNLS equation. We have presented the multipeak soliton and hybrid solutions, both of which are caused by the higher-order effects. All three types of solutions reduced to small localized perturbations of the background at time zero. We have revealed the relationship between the state transition and the linear MI.

Acknowledgements This work has been supported by the National Major Science and Technology Program for Water Pollution Control and Treatment (No. 2017ZX07101-002), by the National Natural Science Foundation of China under Grant Nos. 11305060, 11705145, 11705290 and 61705006 and by the Fundamental Research Funds of the Central Universities (No. 2018MS048) and by China Postdoctoral Science Foundation funded sixtieth batches (No. 2016M602252).

Compliance with ethical standards

Conflict of interest Authors declare that they have no competing interests.

References

1. Wang, L., Zhu, Y.J., Qi, F.H., Li, M., Guo, R.: Modulational instability, higher-order localized wave structures, and nonlinear wave interactions for a nonautonomous Lenells–Fokas equation in inhomogeneous fibers. Chaos **25**, 063111 (2015)
2. Wang, L., Li, X., Qi, F.H., Zhang, L.L.: Breather interactions and higher-order nonautonomous rogue waves for the inhomogeneous nonlinear Schrödinger Maxwell–Bloch equations. Ann. Phys. **359**, 97 (2015)
3. Wang, L., Wang, Z.Q., Sun, W.R., Shi, Y.Y., Li, M., Xu, M.: Dynamics of Peregrine combs and Peregrine walls in an inhomogeneous Hirota and Maxwell–Bloch system. Commun. Nonlinear Sci. Numer. Simul. **47**, 190 (2017)
4. Wang, L., Jiang, D.Y., Qi, F.H., Shi, Y.Y., Zhao, Y.C.: Dynamics of the higher-order rogue waves for a generalized mixed nonlinear Schrödinger model. Commun. Nonlinear Sci. Numer. Simul. **42**, 502 (2017)
5. Aman, S., Khan, I., Ismail, Z., Salleh, M.Z., Al-Mdallal, Q.M.: Heat transfer enhancement in free convection flow of CNTs Maxwell nanofluids with four different types of molecular liquids. Sci. Rep. **7**, 2445 (2017)
6. Khan, I., Shah, N.A., Mahsud, Y., Vieru, D.: Heat transfer analysis in a Maxwell fluid over an oscillating vertical plate using fractional Caputo–Fabrizio derivatives. Eur. Phys. J. Plus **132**, 194 (2017)
7. Khan, I., Gul, A., Shafie, S.: Effects of magnetic field on molybdenum disulfide nanofluids in mixed convection flow inside a channel filled with a saturated porous medium. J. Porous Media **20**, 435 (2017)
8. Khan, I., Shah, N.A., Dennis, L.C.C.: A scientific report on heat transfer analysis in mixed convection flow of Maxwell fluid over an oscillating vertical plate. Sci. Rep. **7**, 40147 (2017)
9. Abdulhameed, M., Khan, I., Vieru, D., Shafie, S.: Exact solutions for unsteady flow of second grade fluid generated by oscillating wall with transpiration. Appl. Math. Mech. **35**, 821 (2014)
10. Khan, A., Khan, I., Ali, F., Shafie, S.: Effects of wall shear stress on unsteady MHD conjugate flow in a porous medium with ramped wall temperature. PloS ONE **9**, e90280 (2014)
11. Khan, I., Ali, F., Shafie, S.: Stokes' second problem for magnetohydrodynamics flow in a Burgers' fluid: the cases $\gamma = \lambda^2/4$ and $\gamma > \lambda^2/4$. PloS ONE **8**, e61531 (2013)
12. Ali, F., Norzieha, M., Sharidan, S., Khan, I., Hayat, T.: New exact solutions of Stokes' second problem for an MHD second grade fluid in a porous space. Int. J. Nonlinear Mech. **47**, 521 (2012)
13. Khan, I., Fakhar, K., Anwar, M.I.: Hydromagnetic rotating flows of an Oldroyd-B fluid in a porous medium. Spec. Top. Rev. Porous Media Int. J. **3**, 89 (2012)
14. Khan, I., Fakhar, K., Sharidan, S.: Magnetohydrodynamic rotating flow of a generalized Burgers' fluid in a porous medium with Hall current. Transp. Porous Media **91**, 49 (2012)
15. Osborne, A.R.: Nonlinear Ocean Waves and the Inverse Scattering Transform. Elsevier, New York (2010)
16. Agrawal, G.P.: Nonlinear Fiber Optics, 3rd edn. Academic-Press, San Diego (2002)
17. Bailung, H., Sharma, S.K., Nakamura, Y.: Observation of Peregrine solitons in a multicomponent plasma with negative ions. Phys. Rev. Lett. **107**, 255005 (2011)
18. Gross, E.P.: Structure of a quantized vortex in boson systems. Il Nuovo Cimento **20**, 454 (1961)
19. Pitaevskii, L.P.: Vortex lines in an imperfect Bose gas. Sov. Phys. JETP **13**, 451 (1961)
20. Zakharov, V.E., Shabat, A.B.: Exact theory of two-dimensional self-focusing and one-dimensional self-modulation of waves in nonlinear media. Sov. Phys. JETP **34**, 62 (1972)
21. Kedziora, D.J., Ankiewicz, A., Akhmediev, N.: Second-order nonlinear Schrödinger equation breather solutions in the degenerate and rogue wave limits. Phys. Rev. E **85**, 066601 (2012)
22. Akhmediev, N., Ankiewicz, A., Soto-Crespo, J.M.: Rogue waves and rational solutions of the nonlinear Schrödinger equation. Phys. Rev. E **80**, 026601 (2009)
23. He, J.S., Zhang, H.R., Wang, L.H., Porsezian, K., Fokas, A.S.: Generating mechanism for higher-order rogue waves. Phys. Rev. E **87**, 052914 (2013)
24. He, J.S., Xu, H., Wang, J., Porsezian, K.: Generation of higher-order rogue waves from multibreathers by double degeneracy in an optical fiber. Phys. Rev. E **95**, 042217 (2017)
25. Wang, L., Zhu, Y.J., Wang, Z.Z., Qi, F.H., Guo, R.: Higher-order semirational solutions and nonlinear wave interactions for a derivative nonlinear Schrödinger equation. Commun. Nonlinear Sci. Numer. Simul. **33**, 218 (2016)
26. Wang, L., Zhang, L.L., Zhu, Y.J., Qi, F.H., Li, M.: Modulational instability, nonautonomous characteristics and semirational solutions for the coupled nonlinear Schrödinger equations in inhomogeneous fibers. Commun. Nonlinear Sci. Numer. Simul. **40**, 216 (2016)
27. Wang, L., Li, M., Qi, F.H., Xu, T.: Modulational instability, nonautonomous breathers and rogue waves for a variable-coefficient derivative nonlinear Schrödinger equation in the inhomogeneous plasmas. Phys. Plasmas **22**, 032308 (2015)
28. Wang, X., Liu, C., Wang, L.: Rogue waves and W-shaped solitons in the multiple self-induced transparency system. Chaos **27**, 093106 (2017)

29. Wang, X., Liu, C., Wang, L.: Darboux transformation and rogue wave solutions for the variable-coefficients coupled Hirota equations. J. Math. Anal. Appl. **449**, 1534 (2017)
30. Wang, X., Wang, L.: Darboux transformation and nonautonomous solitons for a modified Kadomtsev-Petviashvili equation with variable coefficients. Comput. Math. Appl. (2018). https://doi.org/10.1016/j.camwa.2018.03.022
31. Wang, X., Zhang, J.L., Wang, L.: Conservation laws, periodic and rational solutions for an extended modified Korteweg–de Vries equation. Nonlinear Dyn. (2018). https://doi.org/10.1007/s11071-018-4143-z
32. Chabchoub, A., Hoffmann, N., Akhmediev, N.: Rogue wave observation in a water wave tank. Phys. Rev. Lett. **106**, 204502 (2011)
33. Chabchoub, A., Hoffmann, N., Onorato, M., Akhmediev, N.: Super rogue waves: observation of a higher-order breather in water waves. Phys. Rev. X **2**, 011015 (2012)
34. Chabchoub, A., Hoffmann, N., Onorato, M., Slunyaev, A., Sergeeva, A., Pelinovsky, E., Akhmediev, N.: Observation of a hierarchy of up to fifth-order rogue waves in a water tank. Phys. Rev. E **86**, 056601 (2012)
35. Chabchoub, A., Kimmoun, O., Branger, H., Hoffmann, N., Proment, D., Onorato, M., Akhmediev, N.: Experimental observation of dark solitons on the surface of water. Phys. Rev. Lett. **110**, 124101 (2013)
36. Kibler, B., Fatome, J., Finot, C., Millot, G., Genty, G., Wetzel, B., Akhmediev, N., Dias, F., Dudley, J.M.: Observation of Kuznetsov–Ma soliton dynamics in optical fibre. Sci. Rep. **236**, 463 (2012)
37. Frisquet, B., Kibler, B., Millot, G.: Collision of Akhmediev breathers in nonlinear fiber optics. Phys. Rev. X **3**, 041032 (2013)
38. Zakharov, V.E., Gelash, A.A.: Nonlinear stage of modulation instability. Phys. Rev. Lett. **111**, 054101 (2013)
39. Gelash, A.A., Zakharov, V.E.: Superregular solitonic solutions: a novel scenario for the nonlinear stage of modulation instability. Nonlinearity **27**, R1 (2014)
40. Kibler, B., Chabchoub, A., Gelash, A., Akhmediev, N., Zakharov, V.E.: Superregular breathers in optics and hydrodynamics: omnipresent modulation instability beyond simple periodicity. Phys. Rev. X **5**, 041026 (2015)
41. Biondini, G., Fagerstrom, E.: The integrable nature of modulational instability. SIAM J. Appl. Math. **75**, 136 (2015)
42. Biondini, G., Mantzavinos, D.: Universal nature of the nonlinear stage of modulational instability. Phys. Rev. Lett. **116**, 043902 (2016)
43. Qiu, D.Q., He, J.S., Zhang, Y.S., Porsezian, K.: The Darboux transformation of the Kundu–Eckhaus equation. Proc. R. Soc. A **471**, 20150236 (2015)
44. Hirota, R.: Exact envelope-soliton solutions of a nonlinear wave equation. J. Math. Phys. **14**, 805 (1973)
45. Lakshmanan, M., Porsezian, K., Daniel, M.: Effect of discreteness on the continuum limit of the Heisenberg spin chain. Phys. Lett. A **133**, 483 (1988)
46. Porsezian, K., Daniel, M., Lakshmanan, M.: On the integrability aspects of the one-dimensional classical continuum isotropic biquadratic Heisenberg spin chain. J. Math. Phys. **33**, 1807 (1992)
47. Porsezian, K.: Completely integrable nonlinear Schrödinger type equations on moving space curves. Phys. Rev. E **55**, 3785 (1997)
48. Zhang, J.H., Wang, L., Liu, C.: Superregular breathers, characteristics of nonlinear stage of modulation instability induced by higher-order effects. Proc. R. Soc. A **473**, 20160681 (2017)
49. Hoseini, S.M., Marchant, T.R.: Solitary wave interaction and evolution for a higher-order Hirota equation. Wave Motion **44**, 92 (2006)
50. Chowdury, A., Kedziora, D.J., Ankiewicz, A., Akhmediev, N.: Soliton solutions of an integrable nonlinear Schrödinger equation with quintic terms. Phys. Rev. E **90**, 032922 (2014)
51. Wujičić, N., Kregar, G., Ban, T., Aumiler, D., Pichler, G.: Frequency comb polarization spectroscopy of multilevel rubidium atoms. Eur. Phys. J. D **68**, 9 (2014)
52. Chowdury, A., Kedziora, D.J., Ankiewicz, A., Akhmediev, N.: Breather solutions of the integrable quintic nonlinear Schrödinger equation and their interactions. Phys. Rev. E **91**, 022919 (2015)
53. Chowdury, A., Kedziora, D.J., Ankiewicz, A., Akhmediev, N.: Breather-to-soliton conversions described by the quintic equation of the nonlinear Schrödinger hierarchy. Phys. Rev. E **91**, 032928 (2015)
54. Wang, L., Wang, Z.Q., Zhang, J.H., Qi, F.H., Li, M.: Stationary nonlinear waves, superposition modes and modulational instability characteristics in the AB system. Nonlinear Dyn. **86**, 185 (2016)
55. Wang, L., Li, S., Qi, F.H.: Breather-to-soliton and rogue wave-to-soliton transitions in a resonant erbium-doped fiber system with higher-order effects. Nonlinear Dyn. **85**, 389 (2016)
56. Wang, L.H., Porsezian, K., He, J.S.: Breather and rogue wave solutions of a generalized nonlinear Schrödinger equation. Phys. Rev. E **87**, 053202 (2013)
57. Chen, S.H.: Twisted rogue-wave pairs in the Sasa–Satsuma equation. Phys. Rev. E **88**, 023202 (2013)
58. Bandelow, U., Akhmediev, N.: Persistence of rogue waves in extended nonlinear Schrödinger equations: integrable Sasa–Satsuma case. Phys. Rev. A **376**, 1558 (2012)
59. Bandelow, U., Akhmediev, N.: Sasa-Satsuma equation: Soliton on a background and its limiting cases. Phys. Rev. E **86**, 026606 (2012)
60. Chowdury, A., Ankiewicz, A., Akhmediev, N.: Moving breathers and breather-to-soliton conversions for the Hirota equation. Proc. R. Soc. A **471**, 20150130 (2015)
61. Cai, L.Y., Wang, X., Wang, L., Li, M., Liu, Y., Shi, Y.Y.: Nonautonomous multi-peak solitons and modulation instability for a variable-coefficient nonlinear Schrödinger equation with higher-order effects. Nonlinear Dyn. **90**, 2221 (2017)
62. Wang, L., Zhu, Y.J., Wang, Z.Q., Xu, T., Qi, F.H., Xue, Y.S.: Asymmetric Rogue waves, breather-to-soliton conversion, and nonlinear wave interactions in the Hirota–Maxwell–Bloch system. J. Phys. Soc. Jpn. **85**, 024001 (2016)
63. Wang, L., Zhang, J.H., Liu, C., Li, M., Qi, F.H.: Breather transition dynamics, Peregrine combs and walls, and modulation instability in a variable-coefficient nonlinear Schrödinger equation with higher-order effects. Phys. Rev. E **93**, 062217 (2016)
64. Wang, L., Zhang, J.H., Wang, Z.Q., Liu, C., Li, M., Qi, F.H., Guo, R.: Breather-to-soliton transitions, nonlinear wave interactions, and modulational instability in a higher-order

generalized nonlinear Schrödinger equation. Phys. Rev. E **93**, 012214 (2016)
65. Liu, C., Ren, Y., Yang, Z.Y., Yang, W.L.: Superregular breathers in a complex modified Korteweg-de Vries system. Chaos **27**, 083120 (2017)
66. Ren, Y., Wang, X., Liu, C., Yang, Z.Y., Yang, W.L.: Characteristics of fundamental and superregular modes in a multiple self-induced transparency system. Commun. Nonlinear Sci. Numer. Simul. **63**, 161 (2018)
67. Liu, C., Yang, Z.Y., Zhao, L.C., Duan, L., Yang, G., Yang, W.L.: Symmetric and asymmetric optical multi-peak solitons on a continuous wave background in the femtosecond regime. Phys. Rev. E **94**, 042221 (2016)
68. Liu, C., Yang, Z.Y., Zhao, L.C., Yang, W.L.: State transition induced by higher-order effects and background frequency. Phys. Rev. E **91**, 022904 (2015)
69. Liu, C., Yang, Z.Y., Zhao, L.C., Yang, W.L.: Transition, coexistence, and interaction of vector localized waves arising from higher-order effects. Ann. Phys. **362**, 130 (2015)